swissloop

FINAL RESEARCH SUBMISSION

Full-Scale Technical

Manuel Kälin

Assessment of Heat Management Strategies for Hyperloop Pods

Swissloop
Full-scale Technical
Wordcount: 8500 (Excluding sources, appendices and this page)
https://swissloop.ch/research/

Abstract
This thesis deals with the problem of thermal management in a hyperloop pod. The goal is to maintain a constant temperature inside the hyperloop pod. The focus is on heat dissipation from the pod to its environment, namely the tube and the air inside it. The question is whether the dissipated heat is sufficient to keep the temperature constant. At first, some general assumptions are made about the technical characteristics of the hyperloop. Thereof the approximate geometry and properties of the air in the tube are the most important. The different sources of heat in a hyperloop pod are examined. Based on the assumptions the heat transferred by the two modes, radiation and convection, is calculated for the initial input values. The influence of the different input values is examined. The work shows that the initial inputs don't lead to the desired heat dissipation. Improvements are needed. In this work the use of fins and a heat pump is investigated. With the improvements it is possible to have a dissipation in the same range as the heat coming from the heat sources in the passenger cabin (passengers & facilities). Since heat from the passenger cabin is only a part of the thermal management problem for hyperloop pods, further research is needed.

Statement of Contribution

Name	Affiliated with	Chapter number	Contribution
Manuel Kälin	ETH/Swissloop	ALL	Wrote
Emiliano Ivan Maria Casati	ETH	ALL	Gave advice
Manuel Häusler	Eurotube	ALL	Gave advice
Roberto Molinari	Swissloop	ALL	Gave advice

Contents

List of Figures

List of Tables

Nomenclature

Dimensionless Numbers

Kn	Knudsen number (ratio of the molecular mean free path length to a representative physical length scale)	
Ma	Mach number (ratio of flow velocity to the local speed of sound)	
Nu	Nusselt number (ratio of total heat transfer to conductive heat transfer)	
Pr	Prandtl number (ratio of momentum diffusivity to thermal diffusivity)	
Re	Reynolds number (ratio of inertial forces to viscous forces)	

Fluid and Thermodynamics

$\dot{Q}$	heat flow	W
ϵ	emissivity	
γ	heat capacity ratio	
ν	kinematic viscosity	$\mathrm{m^2\,s^{-1}}$
σ	Boltzmann constant	$1.380\,648\,52 \times 10^{-23}\,\mathrm{m^2\,kg\,s^{-2}\,K^{-1}}$
a	speed of sound	$\mathrm{m\,s^{-1}}$
c_d	drag coefficient	
c_p	heat capacity at constant pressure	$\mathrm{W\,kg^{-1}\,K^{-1}}$
c_v	heat capacity at constant volume	$\mathrm{W\,kg^{-1}\,K^{-1}}$

F	force	N
F_{x-y}	view factor	
h	heat transfer coefficient convection	$\mathrm{W\,m^{-2}\,K^{-1}}$
k	thermal conductivity	$\mathrm{W\,m^{-1}\,K^{-1}}$
P	power	W
R	thermal resistance	$\mathrm{m^2\,K\,W^{-1}}$
r	recovery factor	

Other Symbols

β	blockage ratio	
A	area	$\mathrm{m^2}$
L	length (usually pod length)	m
l	fin length	m
u	velocity	$\mathrm{m\,s^{-1}}$

Thermodynamic State Variables

ρ	density	$\mathrm{kg\,m^{-3}}$
p	pressure	$\mathrm{N\,m^{-2}}$
T	temperature	$\mathrm{W\,m^{-2}\,K^{-1}}$

Acronyms

CFD	computational fluid dynamics
COP	coefficient of performance
EHW	european hyperloop week
ETH	Eidgenössische Technische Hochschule
PCM	phase change material

1 Introduction

The publication of Elon Musk's white paper called Hyperloop Alpha in 2013 [14] and the hyperloop competition for student teams that he launched gave a strong boost to research in this area. The idea of a hyperloop is to travel with a pod in a nearly vacuumed tube. The low air resistance allows the pod to travel at very high speeds. The hyperloop concept as a whole presents many technical challenges that need to be overcome in order to realize a commercial system. The thermal management of the hyperloop pod is one of those problems. The majority of hyperloop research focuses on feasibility studies for cost [19] and energy reasons [5] or on the realization of a specific hyperloop route [11]. The aerodynamics of hyperloop pods is the second major topic found in the research [12]. There is no currently known published scientific paper on thermal management of hyperloop pods, but there is a bachelor thesis about thermal management [6] written by a student from the Eidgenössische Technische Hochschule (ETH) in cooperation with Swissloop [4], a team of students from ETH who are building a hyperloop pod prototyp every year. In this work the thermal management was realized using a phase change material (PCM) and the system was also installed in Swissloop's prototyp of the year 2023. However there were significant differences to a full scale hyperloop. The prototype is smaller than a full scale hyperloop and also the operation mode is very different. The maximum speed and the range are much lower. Nevertheless, the work was able to show that heat storage using a PCM cooling module has the potential to be used for heat management in hyperloop pods. A disadvantage of the thermal management using PCM is, that the PCM module which stores the heat must be exchanged during a traveling stop of the hyperloop, because the module doesn't have unlimited heat capacity. Other solutions are therefore desirable. At the european hyperloop week (EHW) 2023 a conceptual feasibility study of hyperloop Vehicle thermal management Systems was presented [8]. This work showed different approaches for the thermal management.

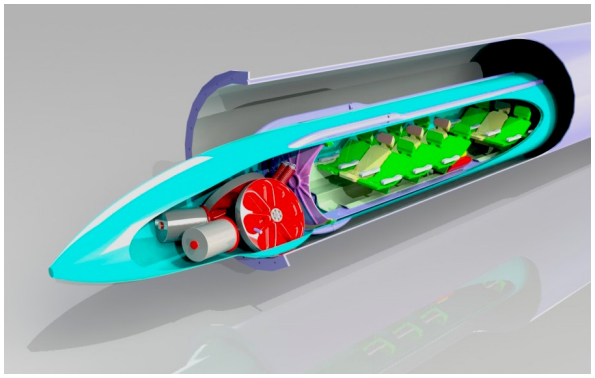

Figure 1.1: hyperloop concept illustration. (Source: https://upload.wikimedia.org/wikipedia/commons/5/59/Hyperloop_pod_Cheetah.JPG, licensed under CC BY-SA 4.0 DEED, downloaded on 22.05.2024)

There are several companies that have set themselves the goal of developing and realizing hyperloops. The two examples are Hardt Hyperloop and Eurotube [2, 3]. These companies however haven't published details about their ideas for thermal management and it is not clear, if they both have concepts how to solve this problem. To dissipate heat there is the widely used mode of convectional heat transfer, which can only be used to a limited extend in a near vacuum environment. Heat radiation is the second way to dissipate heat. Since hyperloops are not the only systems that use radiation for thermal control, there are some sources of information from other applications. In space the only way to dissipate heat is radiation [1]. There are used large radiation panels to dissipate heat. The use of special coatings to improve radiative properties is applied too. Unlike on a spacecraft, in the hyperloop tube there is not a complete vacuum and therefore there is also convectional heat transfer. To make calculations on convectional heat transfer it is important to understand the basics of hyperloop pod aerodynamics [12]. As the hyperloop pod is expected to travel at very high speed and low pressure, the heat transfer varies from the most common convective heat transfer problems. For calculation of convectional heat transfer established literature can be consulted [9, 10]. These two books also describe the other modes of heat transfer and serve as a reference for radiation and conduction. For the radiative heat transfer there is a more detailed book only on radiation [13].

This work is dealing with the thermal management of hyperloop pods. To be more specific the goal is to maintain the temperature in the hyperloop pod at a constant level. To achieve this the heat coming from the heat sources inside the pod needs to be dissipated from the hyperloop pod to its surrounding, meaning the air and the tube. The main question in this work is whether enough heat is dissipated to the surrounding through

convection and radiation, so that the temperature in the system stays in the accepted range.

To do calculations on the heat dissipation at first some assumptions are made. The most important are: the approximate geometry, the air properties in the tube, basic aerodynamics of the hyperloop pod and the temperatures of the components involved in heat transfer. Thermodynamic properties like thermal conductivity and the emissivities as well as the view factors of the radiating surfaces have also to be assumed. Then the heat transfer is calculated and the influence of the different input parameters is investigated by varying the input parameters. In a next step achieved results are used to improve the heat transfer.

2 System Description

2.1 Problem Setting

As mentioned in chapter 1 the temperatures in the hyperloop pod should be kept constant. In fig. 2.1 a simple illustration of the problem is shown.

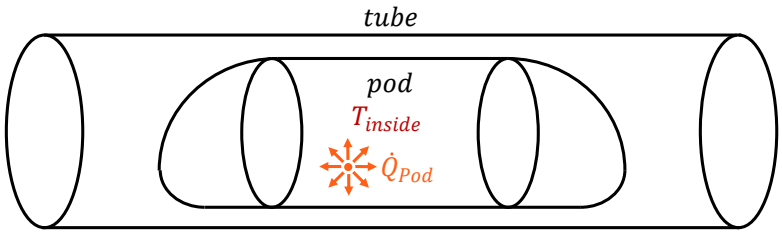

Figure 2.1: Illustration of problem setting. The temperature inside the pod should remain constant, while systems in the pod are heating up the pod. (Source: own illustration)

The most critical temperature is the one of the passenger cabin, which should not exceed $30\,^{\circ}\mathrm{C}$. Friction plays an important rule in the analysis of the heat transfer. Because of the high speeds the air close to the pod surface gets heated up, as it is illustrated in fig. 2.2. This phenomenon is called viscous dissipation and should be considered in the calculations of the heat transfer.

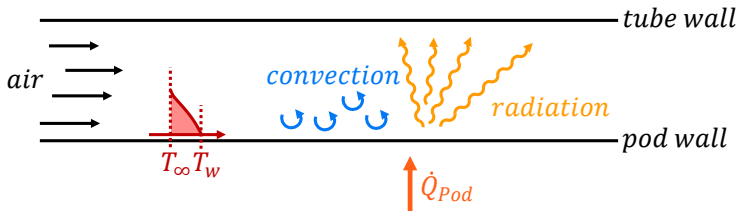

Figure 2.2: Heat transfer between pod and tube. The two modes of heat transfer are convection and radiation. Convection is influenced by viscous dissipation, which is indicated by the red temperature curve in the figure. (Source: own illustration)

2.2 Used Hyperloop Concept

There are a lot of different hyperloop concepts out there. This makes a general analysis difficult. To have a reference the concept used in this work is based on already existing studies. Most of the assumption are from Hardt Hyperloop [3]. Hardt Hyperloop provide relatively detailed values on their full scale hyperloop concept. An overview of the estimated values are presented in table 2.1.

system specification	value	source
cruise speed	$700\,\frac{\mathrm{km}}{\mathrm{h}}/194.44\,\frac{\mathrm{m}}{\mathrm{s}}$	[3]
Mach number	0.57	[3]
pod length	$24\,\mathrm{m}$	[3]
ext. pod diameter	$2.71\,\mathrm{m}$	[3]
inn. tube diameter	$3.5\,\mathrm{m}$	[3]
blockage ratio	0.6	[3]
total weight	$25\,000\,\mathrm{kg}$	[3]
passenger capacity	40	[3]
passenger cabin temperature	$20\,^{\circ}\mathrm{C}$	own ass.
drag force	$3100N$	[3]
power at cruising speed	$665\,\mathrm{kW}$	[3]
motor efficiency	$90\,\%$	[3]
air/tube temperature	$12.5\,^{\circ}\mathrm{C}$	own ass.
air pressure in tube	$1\,\mathrm{mbar}$	[3]

Table 2.1: Hyperloop concept used in this work. Most assumptions are from [3]

For simplicity in the investigation on the heat transfer from the pod to the tube the pod and the tube are estimated to be two cylindrical surfaces into each other. Due to the symmetry a cylindrical shape most likely also has aerodynamic advantages and is used in a lot of hyperloop concepts as an estimation for the geometry. The geometry of the nose and the tail vary in the different studies. Sometimes half spheres are used. In other cases the two ends are some kind of ellipsoids. In this work only the lateral surface is considered.

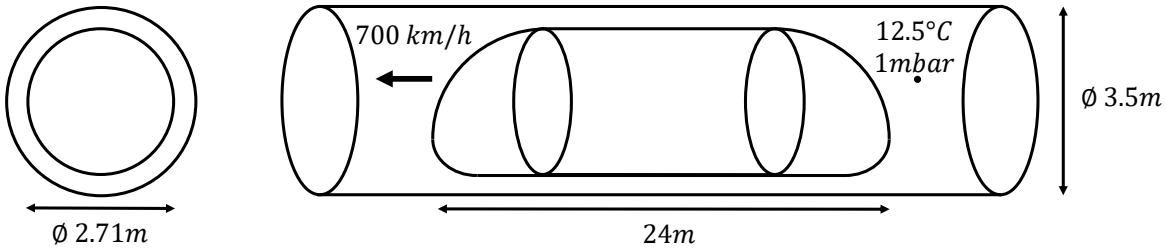

Figure 2.3: Conceptual illustration of the hyperloop concept (Source: own illustration)

The pressure in the tube is $1\,\mathrm{mbar}$. According to [3] it is reasonable to maintain the tube at this pressure. The temperature of the tube and the air inside of it is fixed at $12.5\,^{\circ}\mathrm{C}$ because in a first step the tube is assumed to be underground. In fig. 2.4 a qualitative presentation of the ground temperature is shown. At a depth of about $15\,\mathrm{m}$ the temperature is pretty constant. The value for the temperature is taken from [15], which provides the ground temperature for different cities in the world. The only Swiss city which data is provided for in this source is Lucerne. Therefore the values for Lucerne are used in this work. It is questionable whether a completely underground hyperloop is feasible, because of the high costs. Nevertheless the temperature assumption is used as a starting point. Later, the influence of higher temperatures on the problem can be investigated.

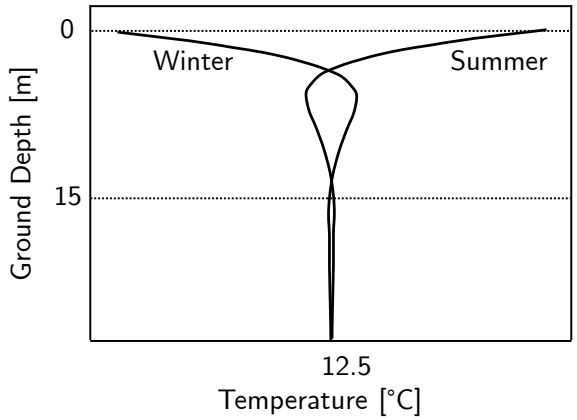

Figure 2.4: Qualitative chart of ground temperature curve (Source: own illustration based on Ouzzane et al. [15], 2015, p.380)

2.3 Air Properties

The aerodynamics and the convectional heat transfer are strongly related to the properties of the air in the tube. To determine the properties temperature and pressure have to be set. As the tube is underground the temperature is assumed to be the same as the ground temperature at the corresponding depth, which is $12.5\,^{\circ}\mathrm{C}$. The pressure in the tube is assumed to be $1\,\mathrm{mbar}$ as shown in table 2.1 and in many other hyperloop concepts.

air properties		
c_p	1443	$\mathrm{J\,kg^{-1}\,K^{-1}}$
c_v	1156	$\mathrm{J\,kg^{-1}\,K^{-1}}$
γ	1.25	$-$
k	0.0253	$\mathrm{W\,m^{-1}\,K^{-1}}$
ρ	0.00122	$\mathrm{kg\,m^{-3}}$
ν	0.0146	$\mathrm{m^2\,s^{-1}}$
Pr	0.708	$-$
a	339	$\mathrm{m\,s^{-1}}$

Table 2.2: Air properties at $12.5\,^{\circ}\mathrm{C}$ and $1\,\mathrm{mbar}$

2.3.1 Flow Regime

Because of the low pressure inside the tube it is necessary to check whether a continuum, approximation holds for the convectional heat transfer or not [12]. When the air in the tube can be treated as continuum the commonly used formulas for convection can be used. To check which approximation holds for the flow, the Knudsen number is calculated. In table 2.3 the correlation between Knudsen number and flow regime is shown [17]. To calculate the Knudsen number eq. (2.1) is used.

$$Kn = \frac{\lambda}{L} = \frac{k_b \cdot T}{\sqrt{2} \cdot d^2 \cdot p \cdot L} \tag{2.1}$$

For the flow around the hyperloop the characteristic length scale of the flow L is assumed to be the gap between pod and tube. In [12] the pod height is used but using the gap makes more sense because the gap is the crucial distance for the heat transfer. Moreover it is also a more conservative assumption than the pod height. The molecular mean free

path λ is calculated with $k_b = 1.3806 \times 10^{-23}\,\mathrm{m^2\,kg\,s^{-2}\,K^{-1}}$ the Boltzmann constant, $d = 3.7 \times 10^{-10}\,\mathrm{m}$ the molecular diameter [12], the temperature $T = 285.65\,\mathrm{K}$ and the pressure $p = 100\,\mathrm{Pa}$. Inserting the values leads to a Knudsen number of 2.9100×10^{-4} which is higher than for normal conditions (about 10^{-7}) but still in the continuum regime.

Knudsen number	flow regime
$Kn < 0.01$	continuum regime
$0.01 < Kn < 0.1$	slip-flow and temperature-jump regime
$0.1 < Kn < 10$	transitional regime
$10 < Kn$	free molecular flow

Table 2.3: The magnitude number of the Knudsen number and corresponding flow regime

2.4 Hyperloop Pod Aerodynamics

The convectional heat transfer and the aerodynamics are strongly related, that's why this section deals with aerodynamics. There are many scientific papers on hyperloop pod aerodynamics. An overview on the research in this area is given in [12]. The aerodynamics of a hyperloop pod are rather complicated and computational fluid dynamics (CFD) simulations have to be done for detailed data on the flow around the hyperloop pod. But some important assumptions about the flow can be made with easier calculations. A 1D isentropic flow analysis shows, that there is a threshold of the pod traveling speed. When this threshold is exceeded the flow gets chocked. This means that the air in front of the pod is pushed like in a piston. Because the air can no longer drain properly, the pressure drag becomes significantly greater. To avoid this, a maximum blockage ratio (β) can be calculated. Most hyperloop concepts don't consider this limit. The material cost for a larger tube are not accepted and therefore to reach the desired cruise speed the limit is exceeded. The blockage ratio used by Hardt [3] and also in this work is $\beta = 0.6$.

$$\beta = \frac{A_{pod}}{A_{tube}} = 0.6 \tag{2.2}$$

Given this blockage ratio, the Mach number at which the pod is traveling at the isentropic limit, can be found solving eq. (2.3).

$$\beta = 1 - Ma_{pod}\left(1 + \frac{\gamma - 1}{2} Ma_{pod}^2\right)^{-\frac{\gamma+1}{2(\gamma-1)}} \left(\frac{\gamma + 1}{2}\right)^{\frac{\gamma+1}{2(\gamma-1)}} \tag{2.3}$$

When comparing the Mach number from the assumptions to the isentropic limit, one can see that it exceeds the limit. The flow state is marked in fig. 2.5 and as it is in the orange region, the flow between the pod and the tube is chocked.

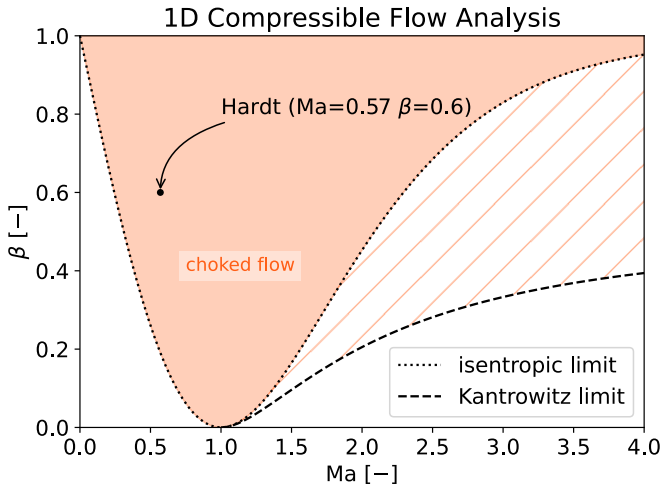

Figure 2.5: Depending on the blockage ratio and the Mach number of the pod, the chart shows whether Ma = 1 is reached in the gap between the pod and the tube or not. Or rather whether the flow gets chocked or not. The boundary between the chocked and the unchocked flow is the isentropic limit. For Ma > 1 there is a second boundary called Kantrowitz limit. Between the two boundaries both, chocked and unchocked flow is possible. (Source: own illustration based on Lang et al. [12], 2024, p.7)

When the isentropic limit is reached or exceeded, the flow in the gap between pod and tube is assumed to be at $Ma = 1$. In the real system there can be shocks in the flow, but this is not considered in this analysis, because it would go beyond the scope of this work. The flow state in the gap between pod and tube is an important information because convectional heat transfer is mainly taking place in this gap. With the Mach number it is possible to calculate other quantities which have to be known for the convectional heat transfer.

With the formulas for compressible flow from [18] the air properties in the gap can be calculated. There are correlations for the case where the pod is traveling under the isentropic limit and the flow in the gap doesn't reach $Ma = 1$ and correlations for the case where the pod is at or over the limit and the flow in the gap reaches $Ma = 1$. In this case

the flow reaches $Ma = 1$ and therefore the properties at this state have to be calculated. These properties are marked with an asterisk in the eqs. (2.4) to (2.7). The properties without asterisks are those which are shown in table 2.2. The two states are connected by Ma_{pod}.

$$\frac{T^*}{T} = \left(\frac{2}{\gamma+1} + \frac{\gamma-1}{\gamma+1}Ma_{pod}^2\right) \tag{2.4}$$

$$\frac{p^*}{p} = \left(\frac{2}{\gamma+1} + \frac{\gamma-1}{\gamma+1}Ma_{pod}^2\right)^{\frac{\gamma}{\gamma-1}} \tag{2.5}$$

$$\frac{\rho^*}{\rho} = \left(\frac{2}{\gamma+1} + \frac{\gamma-1}{\gamma+1}Ma_{pod}^2\right)^{\frac{1}{\gamma-1}} \tag{2.6}$$

$$\frac{a^*}{a} = \left(\frac{2}{\gamma+1} + \frac{\gamma-1}{\gamma+1}Ma_{pod}^2\right)^{\frac{1}{2}} \tag{2.7}$$

The results of the above equations lead to the flow state in the gap. Quantities as c_p, c_v, γ, k, Pr and ν are assumed to be constant.

air properties (crit. state)		
T_*	-8.67	$^\circ\mathrm{C}$
p_*	67.9	Pa
ρ_*	0.000895	$\mathrm{kg\,m^{-3}}$
a_*	326	$\mathrm{m\,s^{-1}}$

Table 2.4: Air properties in the gap between pod and tube

2.4.1 Aerodynamic Drag

The Mach number and the blockage ratio are strongly related to the aerodynamic drag of the pod. Other quantities, such as the length of the pod, play a less important role. In [7] the drag coefficient for a hyperloop pod is derived as a function of the Mach number and the blockage ratio. For these calculations the length of the pod is always 10 times the pod diameter. For the used Geometry this is nearly true, because the diameter of the pod is $2.7\,\mathrm{m}$ and the length is $24\,\mathrm{m}$. By using eq. (2.8) the drag force can be calculated.

$$F_d = \frac{1}{2} \cdot c_d \cdot \rho \cdot A \cdot u_{pod}^2 \tag{2.8}$$

For the drag coefficient the Mach number ($Ma = 0.57$) and the blockage ratio ($\beta = 0.6$) from the general assumptions in section 2.2 are taken to interpolate between the given table values from [7]. The values are the drag coefficient $c_d = 8.56$, the density $\rho = 0.001\,22\,\mathrm{kg\,m^{-3}}$, the frontally projected area of the pod $A = 5.77\,\mathrm{m^2}$ and the speed of the pod $u_{pod} = 194\,\mathrm{m\,s^{-1}}$. Inserting the values from Hardt Hyperloop and the interpolated value for the drag coefficient from [7] leads to an aerodynamic drag of $1134\,\mathrm{N}$. This is in the same order of magnitude as the expected value from Hardt ($1450\,\mathrm{N}$). Although the pressure in the tube is very low, the air resistance is still relevant and can not be neglected. fig. 2.6 shows the drag data from [7].

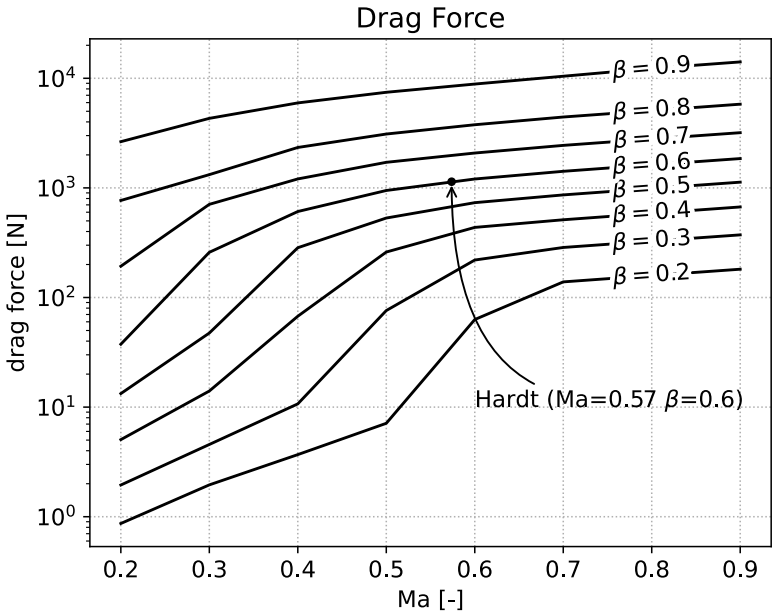

Figure 2.6: Drag Force Data from Bizzozero et al. [7] as a function of the Mach number and the blockage ratio.

2.5 Operation Mode

To estimate the heat sources the major heat sources in a hyperloop pod have to be known. When looking at the predicted energy consumption of a hyperloop system in [16], it is clear

that the aerodynamic and magnetic drag make the biggest contribution to the consumption in the pod. This matches the assumption from Hardt Hyperloop [3] shown in table 2.1. During acceleration the energy consumption is bigger, but some hyperloop concepts use a booster which is mounted on the track to accelerate the pod. For such systems the additional heat from the acceleration is not generated in the pod. In this work the cruising phase is considered, assuming that the acceleration can be powered externally. A detailed analysis of the heat generation is not part of this work, but to compare the values from the heat transfer with some values of the heat generation, simple assumptions are made. For this the main heat sources related to the propulsion and levitation as well as the passengers are considered. The values for the heat sources are shown in table 2.5 as well as some estimations for the maximal allowed operation temperature. This temperatures are important, because for the heat dissipation the temperature at which the heat is generated really matters.

system	critical temperature	heat source
battery	$80\,^{\circ}\mathrm{C}$ or more	N/A
propulsion	$80\,^{\circ}\mathrm{C}$ or more	$81 - 290\,\mathrm{kW}$
levitation & guidance	$80\,^{\circ}\mathrm{C}$ or more	max. $413\,\mathrm{kW}$
passengers & facilities	$30\,^{\circ}\mathrm{C}$	$4 - 30\,\mathrm{kW}$

Table 2.5: Main heat sources in a hyperloop pod. Used equations in appendix A

The used formulas for the heat sources are from [8] and are listed in the appendix A. The calculations in [8] use estimated ranges for the input variables. In the cases where Hardt [3] provides data for an input variable, it is used in the calculations instead of the range in [8]. The values are listed in section 2.2 in table 2.1. When looking at the values of the heat sources in table 2.5 it may well be that these are in those ranges but some of the calculations done in [8] are clearly not reasonable. That's why the value for the battery is missing. Comparing the values of the heat sources to the energy consumption assumed by Hardt ($665\,\mathrm{kW}$) confirms that the numbers in table 2.5 are resonable. When assuming an overall efficiency of the hyperloop of 70% the heat source of the whole system would be $200\,\mathrm{kW}$ which is rather small, but possible in comparison to the values in the table.

To compare the results of the calculation to the heat sources in the system, the heat from the passengers and the facilities is used. In normal operation the temperature of the passengers and the facilities is at $20\,^{\circ}\mathrm{C}$. Further it is assumed that only the upper half of

the pod surface can be used to dissipate the heat, because the electronics and the motor are located in the lower half of the pod. The electronics and the motor can get hotter than the $20\,^{\circ}\mathrm{C}$ and must be insulated, to avoid that they heat up the upper half of the tube with the passengers and the facilities in it. In fig. 2.7 the used pod surface and its temperature are shown.

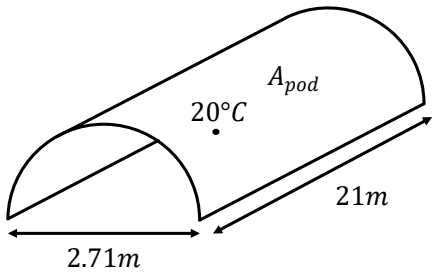

Figure 2.7: Surface area of the pod used for heat transfer. The length is $3\,\mathrm{m}$ shorter than the total pod length, because at the nose and the tail the cross section is smaller. (Source: own illustration)

3 Heat Transfer Model

To model the problem of thermal management in a hyperloop pod and especially the heat transfer from the pod to its surrounding, the heat transfer model in fig. 3.1 is used. The convectional heat transfer is taking place between the pod surface and the air in the tube. The radiation heat is between the pod surface and the tube surface. The whole heat transfer is assumed to take place at steady state.

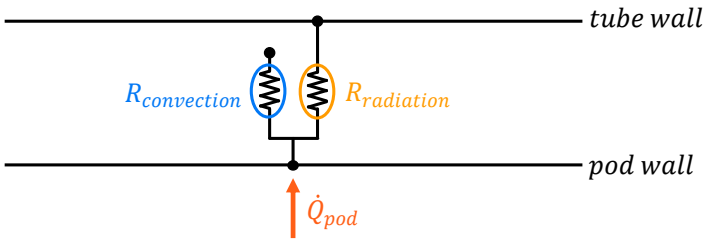

Figure 3.1: Thermal network between pod and tube. Convection takes place from the pod surface to the air and radiation from the pod surface to the tube surface. (Source: own illustration)

The goal of sections 3.1 and 3.2 is to derive a thermal resistance of the corresponding heat transfer mode, so that the heat flow can be calculated dividing the temperature difference by the thermal resistance ($\dot{Q} = \Delta T / R$).

3.1 Radiation

First looking at Radiation, the formulas for diffuse, grey surfaces from [9] are used. The resistance of the radiation in the thermal network can be divided in the three components, which are the three summands of eq. (3.1). This equation holds for two surfaces only seeing each other and nothing else. In the case of the pod and the tube this is an approximation because not the whole pod surface is considered and the ends of the tube are neglected,

but this approximation only results in a very small error. The first and the last term of eq. (3.1) are the so called surface resistances. The second term is the space resistance.

$$R_{radiation} = \frac{1-\epsilon_{pod}}{\epsilon_{pod} A_{pod}} + \frac{1}{A_{pod} F_{pod-tube}} + \frac{1-\epsilon_{tube}}{\epsilon_{tube} A_{tube}} \tag{3.1}$$

The quantities used in eq. (3.1) are the surface areas of the pod A_{pod} and the tube A_{tube}, the emissivities of the pod ϵ_{pod} and the tube ϵ_{tube} as well as the view factor from the pod to the tube $F_{pod-tube}$.

radiation		
A_{pod}	89.39	m^2
A_{tube}	$\approx \infty$	m^2
ϵ_{pod}	0.8	-
ϵ_{tube}	0.8	-
$F_{pod-tube}$	≈ 1	-
$F_{pod-pod}$	≈ 0	-
$F_{tube-tube}$	≈ 1	-
$F_{tube-pod}$	≈ 0	-

Table 3.1: Quantities used for thermal resistance of radiation

The values used in eq. (3.1) are shown in table 3.1. because this is a good approximation and leads to a simplification of eq. (3.1). With a reasonable value for A_{tube} the third term of the equation is negligibly small. In table 3.1 the approximation of a infinitely big tube surface A_{tube} is made. With this approximation the third term of the equation becomes zero. The emissivities are assumed to be 0.8. This value should be reasonable to reach in reality. To improve the heat transfer these values should get as close as possible to one. This can be achieved by putting special coatings on the surface. The emissivity of commonly used materials are also shown in [13]. The view factors are approximated. It is important that they follow the two rules in eqs. (3.2) and (3.3), called summation rule respectively reciprocity. The view factors from table 3.1 satisfy these rules.

$$\sum_{j=1}^{n} F_{i-j} = 1 \tag{3.2}$$

$$A_i F_{i-j} = A_j F_{j-i} \tag{3.3}$$

To calculate the heat flow from the pod to the tube eq. (3.4) is used. In this formula the temperatures of the two participating bodies are used as well as the Boltzmann constant $\sigma = 1.380\,648\,52 \times 10^{-23}\,\mathrm{m^2\,kg\,s^{-2}\,K^{-1}}$. The equation can be rearranged to have a similar expression to calculate the heat flow as for other modes of heat transfer ($\Delta T/R$). In addition, there is a temperature dependent term at the end of the equation.

$$\dot{Q}_{rad} = \frac{\sigma\left(T_{pod}^4 - T_{tube}^4\right)}{R_{radiation}} = \frac{(T_{pod} - T_{tube})}{R_{radiation}} \sigma\left(T_{pod} + T_{tube}\right)\left(T_{pod}^2 + T_{tube}^2\right) \tag{3.4}$$

3.1.1 Radiation Results

To show the dependencies of the radiation heat flow all input variables are fixed except one. The fixed values are taken from table 3.1. The tube and the pod temperature are assumed to be fixed at $12.5\,^{\circ}\mathrm{C}$ respectively $20\,^{\circ}\mathrm{C}$.

Looking at the formulas for radiation from section 3.1 and the input values in table 3.1, we can see that the tube surface is really big and therefore leads to a very small surface resistance for the tube. Since the resistance is small, there is no need to change the surface area of the tube. Changing the emissivity of the tube also has only little influence on the radiation, because of the big tube surface area. The view factor between pod and tube also has influence on the heat transfer, but is pretty close to 1 which is the best possible value. That's why in the results the influence of the tube surface area and emissivity as well as the influence of the view factor are neglected.

The three listed input parameters are more important for the optimization of the heat transfer.

- Pod emissivity: 0.8 (varied from 0.05 to 1.0)
- Pod surface area: $89.39\,\mathrm{m^2}$ (varied from $0\,\mathrm{m^2}$ to $178.78\,\mathrm{m^2}$)
- Pod surface temperature: $20\,^{\circ}\mathrm{C}$ (varied from $12.5\,^{\circ}\mathrm{C}$ to $60\,^{\circ}\mathrm{C}$)

In figs. 3.2 and 3.3 the results calculated with all input variables fixed at the initial values are indicated with a marker. The x-axis of the plot with the varying pod surface in fig. 3.2 is normalized with the initial input, so the marker or the initial input is at 1. As mentioned in section 2.5 the heat production of the passengers and facilities in the passenger cabin

are assumed to be between $4\,\mathrm{kW}$ to $30\,\mathrm{kW}$. In the plot this is indicated with the orange region, although not the whole range is shown.

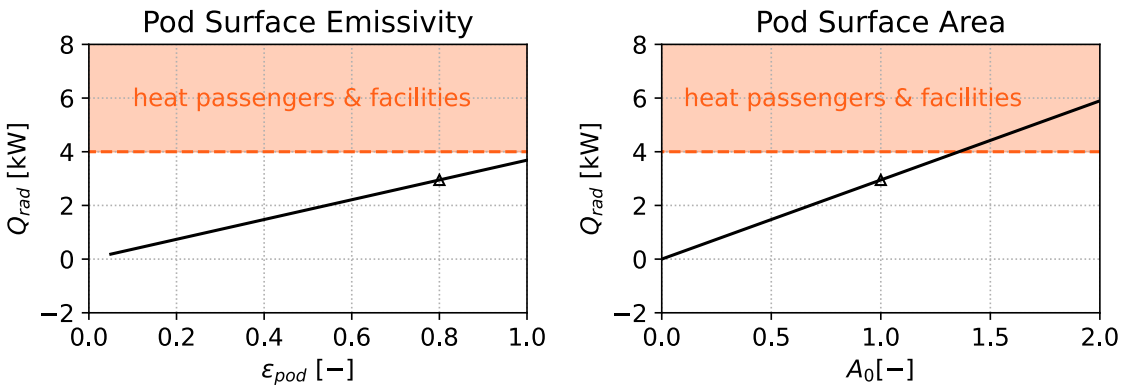

Figure 3.2: Influence of emissivity and surface areas on radiation. The state with the initial input is shown with a marker.

As can be seen in fig. 3.2 the emissivity of the pod influences the heat transfer, but can only reach a maximum of 1. Increasing the pod surface is the second possibility to increase the heat transfer, but this comes with increased friction and therefore also more heating due to friction. Whether increasing the pod surface is reasonable or not, must be investigated in combination with convection, because also convection is influenced by an increased surface. The emissivity and the surface area of the pod are design parameters that can be controlled directly when constructing a hyperloop pod. The pod surface temperature is primarily depending on the temperature of the heat source. As can be seen in fig. 3.3 a increased surface temperature leads to a bigger heat flow. The problem is, that the temperature of the heat source (passengers & facilities) is at low temperature and not in the region of the dashed line.

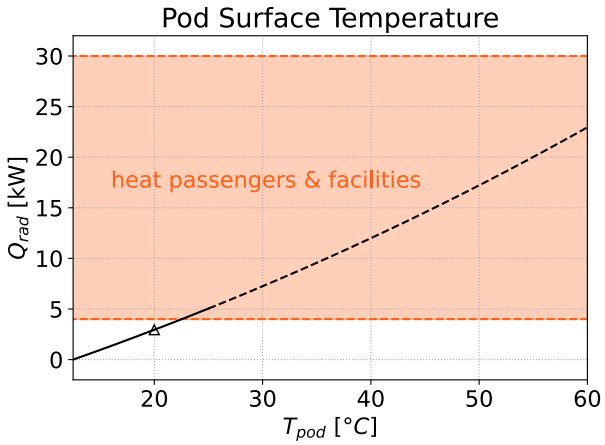

Figure 3.3: Influence of the pod surface temperature on radiation. The initial input state is shown with the marker.

3.2 Convection

As seen in section 2.3.1 the flow can be considered as a continuum. Commonly used formulas for convection should be applicable, but because of the high speed and the low pressure in this case viscous dissipation must be considered. Due to friction in the air near the wall, the air is heated up. To account for that, the calculation of the adiabatic wall temperature is needed. This is the temperature at which the heat flow from the wall to the air is zero. The used equations can be found in [9] which covers the heat transfer at high speeds. Because of the high speed the flow must be considered as compressible and the air properties are very different. The air properties of the free stream used for the calculations are defined in section 2.4 in table 2.4.

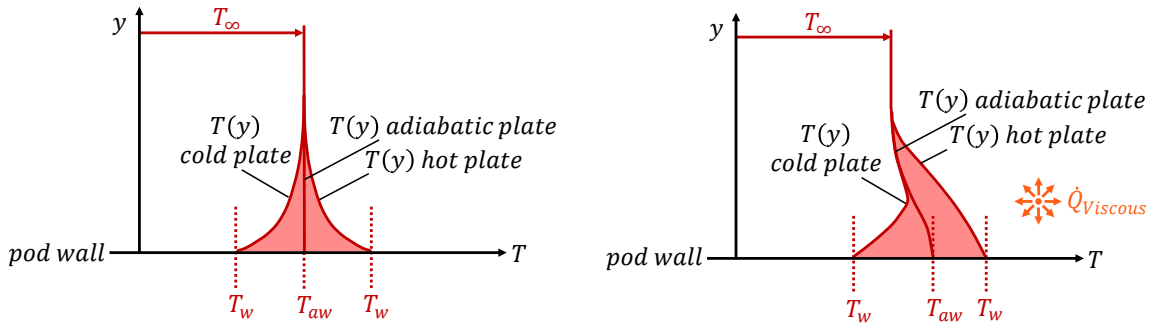

(a) without viscous dissipation

(b) with viscous dissipation

Figure 3.4: Temperature curves of heat transfer with convection for varying distance to wall (y) (Source: own illustration based on Stephan et al. [17], 2019, p.1799)

In fig. 3.4 the first figure shows the convection under normal conditions. The adiabatic wall temperature is the same as the free stream temperature. In the figure also the temperature curve for a hot and a cold plate are shown. The area specific heat transfer can easily be calculated with eq. (3.5). Changing to the case where the velocity of the pod is very high, we can see what happens in fig. 3.4b. The temperature curves are shifted and the adiabatic wall temperature at which no heat flow is present is higher than the air temperature. So due to the friction producing heat, the wall temperature must be higher to have a heat flow from the wall to the air. The heat flow is calculated with eq. (3.6).

no viscous dissipation:
$$\dot{Q} = \overline{h} A \left(T_{pod} - T_\infty\right) \tag{3.5}$$

viscous dissipation:
$$\dot{Q} = \overline{h} A \left(T_{pod} - T_{aw}\right) \tag{3.6}$$

The question is now how to obtain the adiabatic wall temperature. The temperature is defined by the recovery factor r.

$$r = \frac{T_{aw} - T_\infty}{T_0 - T_\infty} \tag{3.7}$$

In the equation T_0 is the stagnation temperature. This temperature can be calculated using eq. (3.8). This temperature is theoretically reached at the point where the velocity is zero. But because the fluid is not brought to rest reversibly, the temperature at the wall is the adiabatic wall temperature and not T_0.

$$\frac{T_0}{T_\infty} = 1 + \frac{\gamma - 1}{2} Ma_\infty^2 \tag{3.8}$$

The recovery factor for gases with Prandtl numbers near unity is defined by eqs. (3.9) and (3.10).

laminar flow: $$r = Pr^{1/2} \tag{3.9}$$

turbulent flow: $$r = Pr^{1/3} \tag{3.10}$$

The Prantl number used for the definition of the recovery factor is evaluated at a state defined by eq. (3.11). So in principle the Prandtl number used in eqs. (3.9) and (3.10) is $Pr = Pr^*$. Because this equation is depending on the adiabatic wall temperature itself, it could be necessary to solve this equations iteratively. As a first assumption the Prandtl number of the stagnation state can be taken.

$$T^* = 0.5\,(T_w - T_\infty) + 0.22\,(T_{aw} - T_\infty) \tag{3.11}$$

The state with the subscribt * describes a reference state which is averaged over the boundary layer. This state is used to calculate the heat transfer coefficient h with the equations known from convection without viscous dissipation. The coefficient can be calculated using the Stanton number St^* or the Nusselt number Nu^*. Here the relations with the Nusselt numbers from eqs. (3.12) and (3.13) are used.

laminar flow: $$Nu_x^* = 0.332 Re_x^{*1/2} Pr^{*1/3} \tag{3.12}$$

turbulent flow: $$Nu_x^* = 0.0296 Re_x^{*4/5} Pr^{*1/3} \tag{3.13}$$

The local heat transfer coefficient is then given by the expression in eq. (3.14). The coefficient is calculated for the laminar and the turbulent case seperatly and must be integrated over the distance x with eq. (3.15) to get an averaged heat transfer coefficient over the corresponding flow state surface. The transition between laminar and turbulent flow is not known for such a specific case with low pressure, high speed and such a geometry. That's why the transition is assumed to be at $Re = 5 \times 10^5$ like for a flat plate.

$$Nu_x^* = \frac{h_x x}{k^*} \tag{3.14}$$

$$\overline{h} = \frac{1}{x_2 - x_1} \int_{x_1}^{x_2} h_x \mathrm{d}x \tag{3.15}$$

Now it is possible to figure out the resistance for the heat transfer of the convection. Assuming that the heat transfer takes place over a length L and that the transition to turbulent flow is at $x_{crit} < L$ we have in fact two resistances in parallel. The total area over which heat is transferred is called A and is divided in the laminar and turbulent part by multiplying with the corresponding fraction, as can be seen in eqs. (3.16) and (3.17)

laminar flow: $$\dot{Q}_{lam} = \overline{h}_{lam} A \frac{x_{crit}}{L} \left(T_w - T_{aw,lam}\right) = \frac{T_w - T_{aw,lam}}{R_{lam}} \tag{3.16}$$

turbulent flow: $$\dot{Q}_{tur} = \overline{h}_{tur} A \frac{L - x_{crit}}{L} \left(T_w - T_{aw,tur}\right) = \frac{T_w - T_{aw,tur}}{R_{tur}} \tag{3.17}$$

Summarizing the heat transfer with viscous dissipation, we can say that it changes the heat transfer coefficient and the temperature at which the heat is dissipated. The heat transfer coefficient is calculated with the quantities of the state with the asterisk subscript. The new temperature at which heat is emitted is not the free-stream temperature anymore, but the adiabatic wall temperature.

It is very difficult to find correlations for the flow around a cylindrical object moving itself in a cylinder. Additionally the flow has to be considered compressible. Here simplification is made by assuming that the lateral pod surface is a flat plate. This assumption ignores some important characteristics of the flow in the gap between pod and tube. The compressibility is accounted for by doing the 1D isentropic flow analysis from section 2.4. But for example the influence of shocks, the influence of the boundary layer on the free stream velocity and the fact that the pod is moving with respect to the tube are ignored. To get more accurate results, the friction coefficients, from a CFD simulation done withing a scientific publication, is used to calculate the convective heat transfer.

3.2.1 Dependency of Friction and Heat Transfer

For the correlations between the friction and convective heat transfer eq. (3.18) can be used. As seen in the equation the averaged quantities are used. The Stanton number St in the equation can be replaced directly with the term that contains the heat transfer coefficient.

$$\begin{aligned} \frac{\overline{C_f}}{2} &= \overline{St} Pr^{2/3} \\ &= \frac{\overline{h}}{\rho c_p u_\infty} Pr^{2/3} \end{aligned} \tag{3.18}$$

To calculate the heat transfer, an averaged adiabatic wall temperature is needed. For that the calculations from section 3.2 can be used.

3.2.2 Convection Results

The calculations for convection are done by using the data from [7]. The data of the friction coefficient are taken directly from the reference. The heat flow in the right chart is calculated by assuming a pod surface temperature of $20\,^{\circ}\mathrm{C}$ and an air temperature of $12.5\,^{\circ}\mathrm{C}$. The results are shown for three different blockage ratios and in a Mach number range of 0.2 to 0.9 for the pod speed.

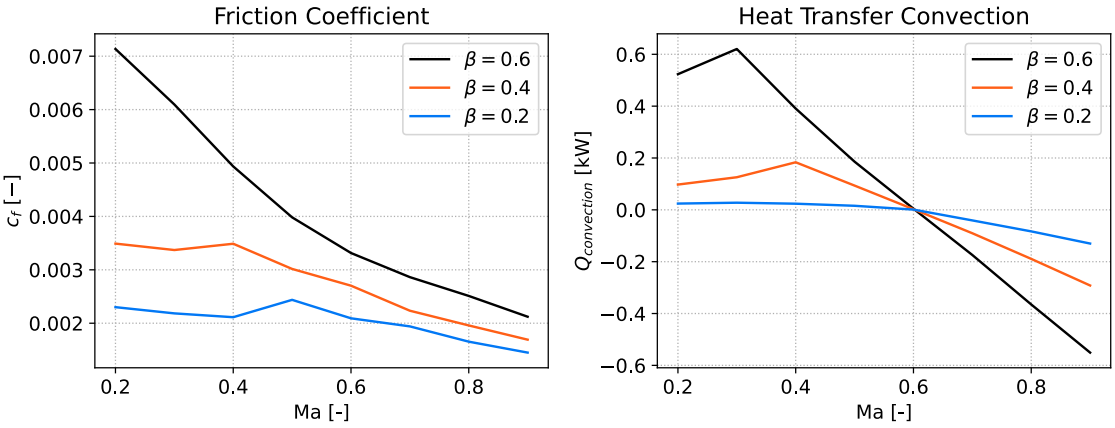

Figure 3.5: The data for the friction from Bizzozero et al. [7] is used to calculate convective heat transfer. On the left side the friction coefficient is shown for different blockage ratios and Mach numbers. On the right side the transferred heat is shown for different blockage ratios and Mach numbers.

As can be seen in the first plot in fig. 3.5 the friction coefficient is clearly higher for bigger blockage ratios. For higher Mach numbers the friction coefficient decreases because the pressure drag makes up the bigger part of the drag force. When comparing the heat transfer in fig. 3.5 it is noticeable that at some point the heat flow is zero for all different blockage ratios at the same time. At this point the adiabatic wall temperature is equal to the pod surface temperature. The adiabatic wall temperature is calculated with the air properties from section 2.4. So the heat flow data is influenced by the calculation on the addiabatic wall temperature. For further calculations a simulation would deliver more accurate results.

Like for radiation the results are calculated for fixed input values and then the influence of different inputs are investigated by varying the input values. The speed of the pod and its geometry have a big influence on the convection. To simplify the problem these values are fixed at the values from table 2.1. Because most of these values are taken from Hardt Hyperloop, it makes sense to compare the results with this hyperloop concept.

Looking at eq. (3.6), the equation for convection with viscous dissipation, we see that the pod surface area and the pod surface temperature are the two variables which can be changed to improve the convective heat transfer, without changing the flow around the pod.

- Pod surface area $89.39\,\mathrm{m}^2$ (varied from $0\,\mathrm{m}^2$ to $178.78\,\mathrm{m}^2$)

- Pod surface temperature $20\,^{\circ}\mathrm{C}$ (varied from $12.5\,^{\circ}\mathrm{C}$ to $60\,^{\circ}\mathrm{C}$)

As for radiation in fig. 3.6 the results calculated with all input variables fixed at the initial values are indicated with a marker. The x-axis of the plot with the varying pod surface in fig. 3.6 is normalized with the initial input, so the marker at the initial input is at 1.

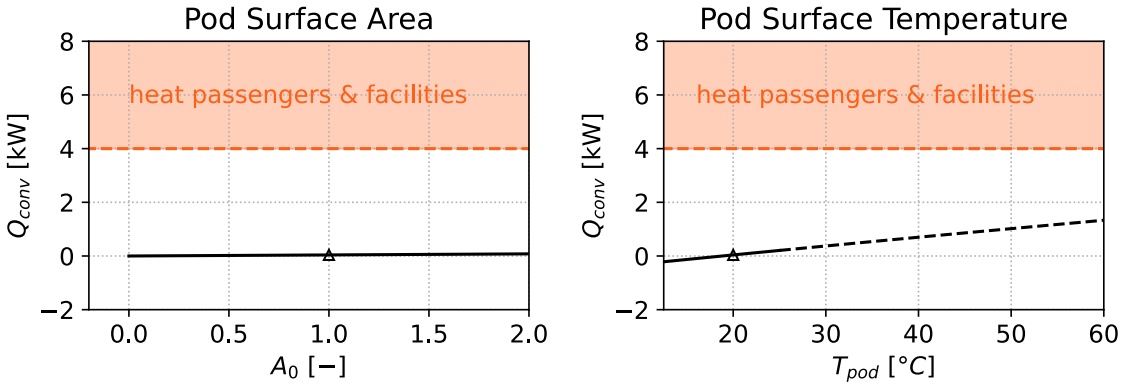

Figure 3.6: Influence of the surface area and the pod temperature on the heat transfer with convection

Because the adiabatic wall temperature is only a bit lower than the initial temperature of the pod surface, the dissipated heat at $20\,^{\circ}\mathrm{C}$ is not substantial. When the pod temperature is lower than the adiabatic wall temperature, the heat flow becomes negative, as can be seen in the second plot of fig. 3.6. The dashed line in fig. 3.6 indicates that the temperature of the heat source has to be increased much more, to increase the heat dissipation significantly.

3.3 Summary Radiation and Convection

The results of the calculations to radiation and convection show, that the heat dissipated by the two heat modes convection and radiation is not high enough with the initial input values.

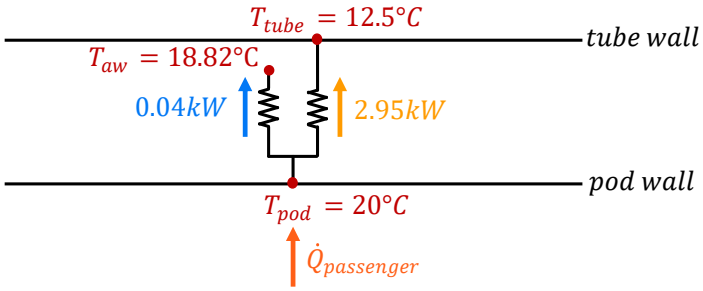

Figure 3.7: Thermal network between pod and tube. Heat dissipated with the two different modes of heat transfer are shown as well as the temperatures. (Source: own illustration)

The total heat dissipated is about $3\,\mathrm{kW}$ and the target range was defined as $4\,\mathrm{kW}$ to $30\,\mathrm{kW}$. It is clearly visible that the radiation makes up the major part of the heat dissipated.

4 Suggestions for improvement

The informations from chapter 3 on how the two considered heat transfer modes change with the inputs help to formulate recommendations for the construction of hyperloop pods and to point out on what future research should focus. In this work two approaches to increase the heat transfer are pursued.

4.1 Fins

The first approach to improve the heat transfer is to put fins on the pod surface. This leads to an increased pod surface and should favour convection and radiation. But more surface area also leads to increased friction. This can not be ignored and should also be included in the evaluation, whether adding fins is a good idea or not.

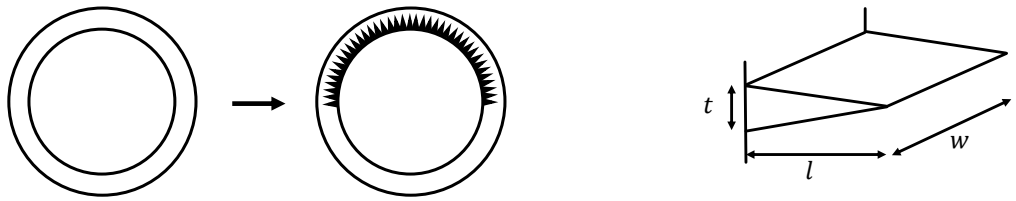

(a) Adding 210 fins to the pod surface (not true to scale) (b) close up of a fin

Figure 4.1: Triangular fins are attached to the pod surface (Source: own illustration)

The triangular fins are placed with w in the longitudinal direction of the pod and t in the circumferential direction. The fins are directly adjoining each other. As a fin material aluminium or copper is common. In this work aluminium is used because it is lighter and less expensive than copper, but has a worse thermal conductivity. The emissivity of aluminium or a coating on the fin surface is not further investigated. The value 0.8 from section 3.1 is used. To calculate the convective heat transfer from a surface covered with fins, formulas

from [10] can be used. First the fin parameter m is calculated. This parameter contains quantities which describe the fin and the flow around it. As indicated in eq. (4.1) the parameter is derived using the convective heat transfer coefficient $\overline{h}$ on the surface, the thermal conductivity of the fin material k and the thickness of the fin t.

$$m = \sqrt{\frac{2\overline{h}}{k \cdot t}} \tag{4.1}$$

The fin parameter is then used to calculate the efficiency of the fin with eq. (4.2). The fin efficiency basically compares the real heat transfer of the fin with the case where the whole fin surface has the temperature of the fin base. It follows that the efficiency approaches one for a surface without fins. For the calculation of the fin efficiency the length of the fin l is used. The two functions $I_1()$ and $I_0()$ are first kind Bessel functions of order one respectively zero. For these functions tabulated values can be found.

$$\eta_f = \frac{1}{ml} \frac{I_1(2ml)}{I_0(2ml)} \tag{4.2}$$

As a next step the thermal resistance of one fin can be calculated. Like for the convective resistance of a flat surface, the fin surface A_f and the heat transfer coefficient for convection $\overline{h}$ are used, as can be seen in eq. (4.3). In addition the fin efficiency from eq. (4.2) is used.

$$R_{fin} = \frac{1}{\eta_f A_f \overline{h}} \tag{4.3}$$

Because the whole fin surface is basically a parallel connection of equal fins, the total thermal resistance is the resistance of one fin divided by the number of fins.

$$R_{fins} = \frac{R_{fin}}{N} \tag{4.4}$$

As a next step calculations on the use of aluminium fins in the case of this work are done. The results are shown in fig. 4.2. In this plot the number of fins on the surface is fixed at 210. Because the fins are adjoining each other, the fin thickness t follows directly from the number of fins. In this case the thickness is $20\,\mathrm{mm}$. By varying the fin length L the total surface can be influenced. In fig. 4.2 the fin length is varied from $0\,\mathrm{mm}$ to $20\,\mathrm{mm}$. On the y-axis the dissipated heat at the corresponding fin length is shown. The x-axis shows the

fin surface area. Because the axis is normalized by the surface area of the pod without fins, the total heat dissipated without fins is at 1. This is also indicated with the marker. The calculations without fins use the same input values as the initial inputs from sections 3.1.1 and 3.2.2. As for the results of convection and radiation the orange band indicates the heat production of the passengers and the facilities.

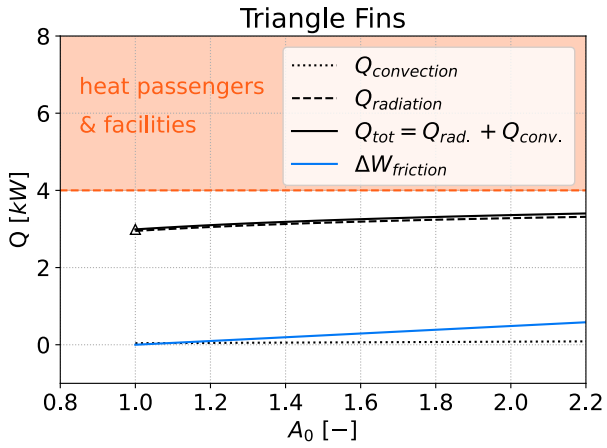

Figure 4.2: The influence of fins on heat dissipation is shown. There is a fixed amount of fins for which the length is increased from 0 on. In the plot the increasing fin surface is shown on the x-axis. Again the marker indicates the state with the initial inputs (e.g. no fins). The blue line is the additional friction due to the increased surface

The total heat dissipated is increasing only little, with growing surface area. However convection and radiation are increased both. The blue line in the plot indicates the additional friction caused by the bigger surface area. The additional power needed with the biggest increase of surface area shown in the plot is about $0.6\,\mathrm{kW}$. In comparison to the whole drag force, which is $603\,\mathrm{kW}$ (including also magnetic drag), this is very small. But it's always a trade-off of heat dissipation and friction and at some point the friction could be increased more than the heat dissipation. You can see, that convection doubles roughly when the surface is also doubled. Unlike the calculations on radiation in section 3.1.1 the radiative heat transfer is not doubled for a surface area increased by a factor of about two. This is because the fins are not flat. By adding fins the base area is not changed. In eq. (4.5) and fig. 4.3 the influence of fin surface area on radiation is presented [9].

$$\epsilon_{fin} = \frac{\epsilon \cdot A_f}{A_b + \epsilon(A_f - A_b)} \tag{4.5}$$

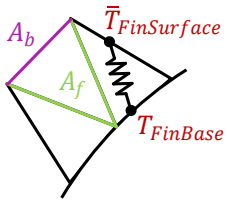

Figure 4.3: Fins change the emissivity and the surface temperature (Source: own illustration)

We can conclude from this formula that the emissivity approaches 1 when the base area gets really small in comparison to the fin area. But to calculate the heat transfer the base area of the fins is used, and therefore the relevant surface is not really increased by adding fins. In section 3.1.1 a emissivity of 0.8 is taken. The emissivity can be maximally increased to a value of 1. In addition the average fin surface temperature is lower than the base temperature. This also impedes the radiative heat transfer. To calculate the average fin surface temperature the fin efficiency can be used, because as mentioned, it relates the fin base temperature with the average fin surface temperature. It is important to use the absolute temperature in Kelvin to get to the correct result.

4.2 Heat Pump

To add a heat pump to the system should increase the pod surface temperature, while the inside remains at a comfortable room temperature. Adding the heat pump leads to the need of an insulated pod wall. Moreover the heat pump consumes electric power. You can make easy calculations for the whole hyperloop pod. Like in section 2.5 the overall efficiency of 70% and the total power consumption of $665\,\mathrm{kW}$ are assumed. The heat production would reach $200\,\mathrm{kW}$. A heat pump with coefficient of performance (COP) of 4 would have to spend $50\,\mathrm{kW}$. In fig. 4.4 the thermal network with the heat pump and the insulation is shown.

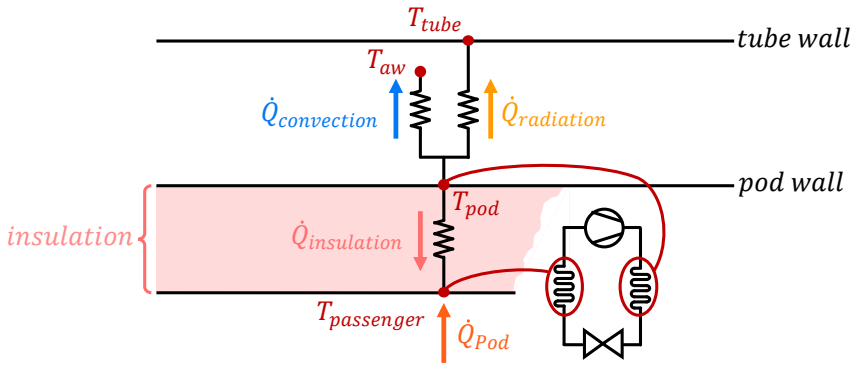

Figure 4.4: Thermal network between pod and tube with heat pump added (Source: own illustration)

As well as added fins, the heat pump generates undesired heat which must be removed from the pod. The ideal COP of a heat pump for cooling is calculated with the fraction of the temperatures (T_h, T_c) shown in eq. (4.6). The subscribt "c" stands for cooling, and the "h" for heating. In this case the passenger cabin is cooled and the pod wall is heated. Because a real heat pump doesn't have an ideal COP, the fraction of the ideal heat pump COP is multiplied by 0.6. The equation also shows the other definition of the COP which is the cooling power Q_c divided by the input power W_{HP} of the heat pump. T_h is chosen $5\,°\mathrm{C}$ hotter and T_c is chosen $5\,°\mathrm{C}$ colder than the desired temperatures for pod wall respectively passenger cabin. This is due to heat transfer in the evaporator and the condenser, which needs to be driven by a temperature difference between the fluid and the heated or cooled environment.

$$COP_{HP} = \frac{\dot{Q}_c}{W_{HP}} = 0.6 \cdot \frac{T_c}{T_h - T_c} \tag{4.6}$$

As mentioned, the pod wall needs an insulation when adding a heat pump. The heat flowing back from the pod wall into the passenger cabin must also be accounted for. This is done by calculating this heat flow and adding it to the needed cool power Q_c. The insulation is assumed to be a half tube, with a thickness of $5\,\mathrm{cm}$ and a thermal conductivity of $0.03\,\mathrm{W\,K^{-1}\,m^{-1}}$. The formula for thermal conductivity in a cylindrical body is defined by eq. (4.7). Choosing the pod diameter as the outer diameter, the inner diameter two times $5\,\mathrm{cm}$ smaller and the pod length as L leads to the thermal resistance of a full tube. Because the considered case is a half tube, the resistance has to be multiplied by 2.

$$R_{cylindrical} = \frac{ln\left(d_{outer}/d_{inner}\right)}{2\pi kL} \tag{4.7}$$

Dividing the temperature difference between the inside of the pod and the pod wall by the thermal resistance leads to the additional cooling needed because of back flowing heat. The energy balance around the heat pump results in eq. (4.8) with the heat flow and power going into the system on the left side and the heat flow going out on the right side.

$$\dot{Q}_c + W_{HP} = \dot{Q}_h \tag{4.8}$$

The result of the heat transfer with a heat pump are shown in fig. 4.5. As in every plot the initial state of the inputs is shown with the marker. The orange range indicates the possible heat production of the passengers and facilities, both located in the passenger cabin.

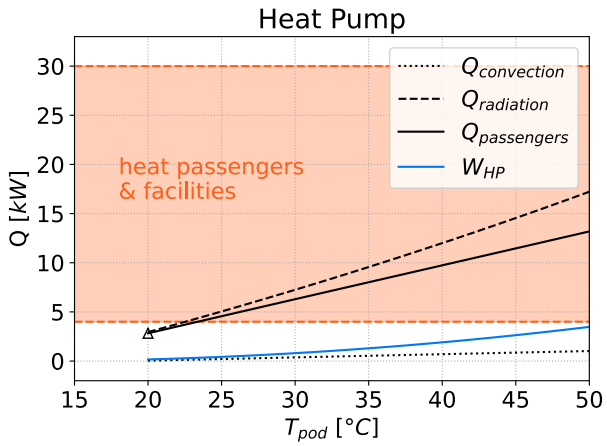

Figure 4.5: Heat transfer with heat pump added to the thermal network. The marker indicates the state with the initial inputs. The heat pump increases the temperature (x-axis) and therefore the dissipated heat from the passengers rises. The blue line indicates the additional power needed to operate the heat pump.

As can be seen in fig. 4.5 the heat pump increases the pod surface temperature. In the plot a range between $20\,^{\circ}\mathrm{C}$ and $50\,^{\circ}\mathrm{C}$ is shown. $Q_{passengers}$ stands for the heat (passengers & facilities) which can be dissipated. This value is lower than radiation and convection added up, because according to the energy balance of the heat pump in eq. (4.8) the cooling $\dot{Q}_c$ is smaller than the heating $\dot{Q}_h$. The blue line shows the needed power for the operation of the heat pump. The additional energy consumption has to be covered by the onboard battery.

5 Conclusion

The problem presented in this work is a contribution to the thermal management of hyperloop pods. To carry passengers in the pod and to ensure the functionality of the technical components of the system it is important, that the temperature stays at a constant level and doesn't exceed the system-specific limit. To do so, the heat from the heat sources in the hyperloop pod must be dissipated. The main heat sources in the hyperloop pod are:

- the battery
- propulsion
- levitation and guidance
- passengers and facilities

The main research question addressed in this paper is whether it is possible to dissipate enough heat with radiation and convection to maintain the temperature of the passenger cabin at a constant value of $20\,^{\circ}\mathrm{C}$. The heat coming from the sources in the passenger cabin is $4\,\mathrm{kW}$ to $30\,\mathrm{kW}$. The heat sources are the passengers and the facilities. The assumptions describing the system used for the calculations are explained in chapter 2. In conclusion I observed, that:

1. With the initial input values assumed in chapter 2 the heat dissipation is only about $3\,\mathrm{kW}$. This is not in the desired range of $4\,\mathrm{kW}$ to $30\,\mathrm{kW}$. With the initial values heat dissipation through radiation is 70 times higher than heat dissipation through convection.
2. In a second step fins are added to the pod surface. Fins have in particular a favourable impact on the convective heat transfer. Because the heat dissipated by convection is really small ($0.04\,\mathrm{kW}$) with the initial values, the impact is not really high. The convection can be doubled with twice the initial surface area when fins are used. But the value of dissipated heat is still only $0.08\,\mathrm{kW}$. With fins attached to the surface the

heat dissipated through radiation can be improved as well but maximally 25%. The fins would have a much higher impact if the temperature of the emitting surface (pod outer surface) was higher. The additional heat dissipated with fins through convection and radiation is about $0.5\,\mathrm{kW}$ and doesn't reach the desired range. Moreover the additional power consumption for propulsion due to friction caused by the bigger surface is also about $0.5\,\mathrm{kW}$. In other words the fins have an efficiency of about 1.0.

3. As another possibility to dissipate more heat, a heat pump is added to the system. The heat pump cools the passenger cabin and at the same time it heats up the outer pod surface, which dissipates heat to the surrounding. The passenger cabin must be insulated to avoid heat flowing from the heated up pod surface into the passenger cabin. With a heat pump it is possible to get a heat dissipation of about $13\,\mathrm{kW}$. This value is in the range of $4\,\mathrm{kW}$ to $30\,\mathrm{kW}$ and can possibly be high enough to dissipate the heat from the passengers and the facilities. To dissipate $13\,\mathrm{kW}$ the heat pump needs to increase the temperature of the outer pod surface to $50\,^{\circ}\mathrm{C}$. To operate the heat pump about $4\,\mathrm{kW}$ are used, so the heat pump has a efficiency of 3.
4. A high surface temperature is needed to dissipate as much heat as possible. As mentioned the heat pump is used to rise the surface temperature. But the efficiency of the heat pump decreases the higher the difference in temperature over the heat pump gets. If there is a turning point, where the efficiency of the heat pump starts decreasing due to rising temperature, it could be an advantage to use fins in addition. This because the additional energy, used by the fins due to more friction, doesn't increase significantly with rising temperatures.
5. By comparing the additional power used to maintain the heat pump ($4\,\mathrm{kW}$) to the overall power consumption assumed by Hardt as $665\,\mathrm{kW}$ [3], it is determined that the power needed for the heat pump doesn't have a high impact on energy consumption.

5.1 Outlook

Effort in further research should be put into the calculations of more accurate values on the heat sources. The work of De Wit and Terpstra [8] and also the work done by Manuel Häusler from Eurotube [2] are fundamental in this area. Moreover the viscous dissipation needs to be examined more closely to understand better how it influences convection. In this work the heat dissipation was always compared with the heat source of the passengers

and the facilities. The electronic components clearly make up the major part of the heat production. In further research the cooling of other heat sources needs to be covered. The fact, that electronics can bear much higher temperatures during operation, than $20\,^{\circ}\mathrm{C}$ facilitates heat dissipation. Furthermore they can be made vacuum compatible and placed such, that there is not much heat flowing from the electronics into the passenger cabin.

Bibliography

[1] Small spacecraft technology state-of-the-art. Technical report, NASA. URL https://www.nasa.gov/smallsat-institute/sst-soa/thermal-control/.

[2] Eurotube. URL https://eurotube.org/.

[3] Hardt hyperloop. URL https://www.hardt.global/.

[4] Swissloop. URL https://swissloop.ch/?lang=de.

[5] Effect of Hyperloop Technologies on the Electric Grid and Transportation Energy. Technical report, Office of Scientific and Technical Information (OSTI), Jan. 2021. URL https://www.osti.gov/biblio/1773025.

[6] T. Aebersold. Design, symulation and manufacturing of a phase change cooling module for low-pressure applications. URL https://swissloop.ch/wp-content/uploads/2023/07/Swissloop_PhaseChangeCooling_RS.pdf.

[7] M. Bizzozero, Y. Sato, and M. A. Sayed. Aerodynamic study of a hyperloop pod equipped with compressor to overcome the kantrowitz limit. 218:104784. ISSN 0167-6105. doi: 10.1016/j.jweia.2021.104784.

[8] L. De Wit and T. Terpstra. Conceptual feasibility study of hyperloop vehicle thermal management systems. URL https://hyperloopconnected.org/2023/06/report-conceptuafeasibility-study-of-hyperloop-vehicle-thermal-management-systems/.

[9] J. P. Holman. *Heat transfer*. McGraw-Hill series in mechanical engineering. McGraw-Hill, 10 edition. ISBN 9780073529363.

[10] F. P. Incropera, D. P. Dewitt, T. L. Bergman, and A. S. Lavine. *Fundamentals of heat and mass transfer*. Wiley, 6 edition. ISBN 9780471457282.

[11] B. Kowal, R. Ranosz, M. Kłodawski, R. Jachimowski, and J. Piechna. Demand for Passenger Capsules for Hyperloop High-Speed Transportation System-Case Study From Poland. *IEEE Transactions on Transportation Electrification*, 8(1):565–589, Mar. 2022. ISSN 2332-7782. doi: 10.1109/TTE.2021.3120536. URL https://ieeexplore.ieee.org/document/9576500.

[12] A. J. Lang, D. P. Connolly, G. de Boer, S. Shahpar, B. Hinchliffe, and C. A. Gilkeson. A review of Hyperloop aerodynamics. 273:106202. ISSN 0045-7930. doi: 10.1016/j.compfluid.2024.106202. URL https://www.sciencedirect.com/science/article/pii/S0045793024000343.

[13] M. F. Modest. *Radiative Heat Transfer*. Elsevier, third edition. ISBN 9780123869449. doi: 10.1016/c2010-0-65874-3. URL https://www.sciencedirect.com/book/9780123869449/radiative-heat-transfer. Print version record.

[14] E. Musk. Hyperloop alpha. URL https://www.tesla.com/sites/default/files/blog_images/hyperloop-alpha.pdf.

[15] M. Ouzzane, P. Eslami-Nejad, M. Badache, and Z. Aidoun. New correlations for the prediction of the undisturbed ground temperature. 53:379–384. ISSN 0375-6505. doi: 10.1016/j.geothermics.2014.08.001. URL https://www.sciencedirect.com/science/article/pii/S0375650514000984.

[16] G. Pareschi, J. Ehwald, N. Leng, B. Paul, and B. Guo. Potential analysis for vacuum transport technologies in public transport in switzerland. URL https://www.aramis.admin.ch/Default?DocumentID=71265&Load=true.

[17] P. Stephan, S. Kabelac, M. Kind, D. Mewes, K. Schaber, and T. Wetzel. *VDI-Wärmeatlas: Fachlicher Träger VDI-Gesellschaft Verfahrenstechnik und Chemieingenieurwesen*. Springer Berlin Heidelberg. ISBN 9783662529898. doi: 10.1007/978-3-662-52989-8.

[18] F. M. White. *Fluid mechanics*. McGraw-Hill Series in Mechanical Engineering. McGraw-Hill, 7 edition. ISBN 9780077422417. Auf der DVD-ROM-Beil. (Student Resource DVD): Engineering Equation Solver (EES).

[19] A. Zenklusen. Modeling the operating costs of an hyperloop connection from zurich to paris. URL https://swissloop.ch/wp-content/uploads/2023/07/Modeling-the-operating-costs-of-Hyperloop.pdf.

A Heat Source Calculations

The used formulas for the heat production are from [8]. Detailed calculation on the heat production in a hyperloop pod can be found there, but the formulas used to calculate the values in table 2.5 are shown in the following. The calculations in [8] use estimated ranges for the input variables. In the cases where Hardt [3] provides data for an input variable, it is used in the calculations instead of the range in [8]. The values are listed in table 2.1.

$$P_{motor} = F_{drag} \cdot u_{pod} \tag{A.1}$$

$$\dot{Q}_{motor} = \frac{1 - \eta_{motor}}{\eta_{motor}} P_{motor} \tag{A.2}$$

$$\dot{Q}_{motor\ drive} = \frac{1 - \eta_{motor\ drive}}{\eta_{motor\ drive} \cdot \eta_{motor}} P_{motor} \tag{A.3}$$

$$\dot{Q}_{propulsion} = \dot{Q}_{motor} + \dot{Q}_{motor\ drive} \tag{A.4}$$

$$\dot{Q}_{levitation} = m \cdot \dot{q}_{levitation} \tag{A.5}$$

$$P_{propulsion} = \frac{P_{motor}}{\eta_{motordrive} \cdot \eta_{motor}} \tag{A.6}$$

$$\dot{Q}_{power} = (P_{propulsion} + P_{levitation})^2 \frac{\overline{R}_{int}}{V_{power}} \tag{A.7}$$

$$\dot{Q}_{passengerscabin} = n \cdot \dot{Q}_{person} + \dot{Q}_{facilities} \tag{A.8}$$